Eur Biophys J (1988) 16:177–185

European Biophysics Journal

The superstructure of chromatin and its condensation mechanism

V. Effect of linker length, condensation by multivalent cations, solubility and electric dichroism properties

M. H. J. Koch [1], Z. Sayers [1], A. M. Michon [1], R. Marquet [2], C. Houssier [2], and J. Willführ [3]

[1] European Molecular Biology Laboratory, c/o DESY, Notkestrasse 85, D-2000 Hamburg 52, Federal Republic of Germany
[2] Laboratoire de Chimie Macromoleculaire et Chimie Physique, Sart Tilman (B6), Université de Liège, B-4000 Liège, Belgium
[3] Biologische Anstalt Helgoland, Notkestrasse 31, D-2000 Hamburg 52, Federal Republic of Germany

Received December 22, 1987/Accepted March 9, 1988

Abstract. Comparison between the internucleosomal distance found by X-ray solution scattering for chicken erythrocyte (23 nm) and sea urchin (30 nm) chromatin indicates that this distance is proportional to the linker length. The diameter of the condensed sea urchin chromatin fibers is about 45 nm which is significantly larger than in chicken erythrocyte chromatin (35 nm). Trivalent cations (Gd, Tb, Cr) and the polyamines spermine and spermidine were found to induce compaction at much lower concentrations than the divalent cations but Gd, Tb and Cr induce aggregation before full compaction of the fibers. The influence of hydrogen bonding is illustrated by comparison of the effects of NaCl, ammonium chloride and alkylammonium chlorides on condensation. Solubility experiments indicate that there is a nearly linear dependence of the Mg^{++} concentration at which precipitation occurs on chromatin concentration and confirm the differences between cations observed by X-ray scattering.

The chicken erythrocyte chromatin samples were further characterized by their reduced electric dichroism. The values found are consistent with the model derived from X-ray scattering and are compared with those reported in the literature.

Key words: X-ray solution scattering, synchrotron radiation, sea urchin chromatin, solubility, condensation, electric dichroism

Introduction

In a series of previous papers (Perez-Grau et al. 1984; Bordas et al. 1986a, b; Koch et al. 1987a, b), a model of the in-vitro structure of chromatin and its condensation mechanism was developed. (For a review of the various models of chromatin structure, see Sayers 1988). At low ionic strength, the structure consists of an irregular chain of nucleosomes connected by straight linker DNA. This structure gives rise in the electron microscope to the zig-zag described by Thoma et al. (1979), which corresponds, even at low resolution, to a filament with outer diameter 25–30 nm. In the absence of the H1/H5 histones this superstructure is not maintained (Thoma et al. 1979; Bordas et al. 1986a). This observation has been recently confirmed and extended by neutron scattering and reconstitution experiments (Gerchman and Ramakrishnan 1987). This view provides a basis for a satisfactory explanation of what are discrepancies in some of the hydrodynamic properties (Ramsay-Shaw and Schmitz 1976; Ausio et al. 1984) when the structure is described as a "10 nm" filament.

The model implies that the average separation between nucleosomes should have a narrow distribution around a value that is proportional to the linker length. Experiments, reported below, on sea urchin chromatin which has a linker that is about 25 base pairs longer than chicken erythrocyte chromatin confirm this. At increasing ionic strength a very rapid equilibrium corresponding to a more compact structure is established in a continuous fashion, leading finally to the formation of the so-called "30 nm" filament described by Finch and Klug (1976). In the latter the short range order packing of the nucleosomes gives rise to characteristic interference bands in the diffraction pattern of oriented fibers (Widom and Klug 1985) which give unambiguous evidence about the preferential orientation of the nucleosomes. The irregular nature of the partially condensed fibers has also been established by electron microscopy (Subirana et al. 1985). The cation concentrations at which compaction of the fiber and precipitation occur, depend on the nature of the cation as well as on chromatin concentration. In this context, the effects of various cations (NH_4^+, NMe_4^+, NEt_4^+, Cr^{3+}, Gd^{3+} and Tb^{3+}, spermine and spermidine) on the compaction and solubility of chicken erythrocyte chromatin was investigated to obtain a more complete picture of the interactions involved.

One of the outstanding problems in chromatin structure concerns the path of the linker. This problem has been addressed by several groups using electric and flow dichroism methods with chromatin from various sources. A survey of the literature indicates, however, that the results from different laboratories are not consistent. We present results of electro-optical measurements on our chicken erythrocyte chromatin samples which indicate that in the condensed form the linker DNA must lie essentially in the plane perpendicular to the fiber axis, in agreement with the X-ray scattering model.

Materials and Methods

Preparation of chromatin fragments from chicken erythrocytes

The preparation of solutions of chromatin fragments containing on average 70 to 90 nucleosomes in TE buffer (5 m*M* *Tris* · HCl, 1 m*M* Na EDTA, 0.1 m*M* Phenylmethylsulfonyl fluoride (PMSF), pH 7.5) followed procedures described earlier (Bordas et al. 1986a). The digested nuclear pellet was washed in 150 m*M* NaCl, 10 m*M* *Tris* · HCl pH 7.5, 1 m*M* EDTA, 0.5 m*M* PMSF and resuspended in 1 volume of this buffer. Chromatin was extracted at about 10 mg DNA/ml by immediately mixing this suspension with about 7 volumes of TE buffer.

Preparation of sea urchin sperm, nuclei and chromatin

Sperm from Mediterranean sea urchins (*Paracentrotus lividus*) obtained from Messrs Stevenino (Cannes, France) at the end of March was collected with a Pasteur pipette by stabbing directly into the gonads of freshly dissected animals. The concentrated sperm was diluted in at least five times the volume of an artificial sea water (ASW) solution consisting of 0.42 *M* NaCl, 9 m*M* KCl, 9.3 m*M* $CaCl_2$, 22.9 m*M* $MgCl_2$, 25.5 $MgSO_4$, 2.15 m*M* $NaHCO_3$. The suspension was filtered through four layers of gauze and centrifuged for 5 min at 200 *g*. The supernatant was centrifuged for 10 min at 700 *g* to collect the sperm. The sperm pellet was washed three times in the same volume of ASW as the first dilution. The final pellet was resuspended in a small volume of ASW and split in aliquots of 2 ml which were carefully mixed with 3 ml of glycerol. These samples in plastic tubes were rapidly frozen in a mixture of acetone and dry ice and stored at −70 °C.

For the preparation of nuclei, the samples were thawed and diluted to obtain five times the original volume (sperm + glycerol) in a solution containing 0.25 *M* sucrose, 50 m*M* *Tris* · HCl pH 7.5, 2 m*M* $MgCl_2$, 1% Triton X-100 and 0.5 m*M* PMSF. Microscopic observation indicates that the solution already contains a large amount of free tails at this stage. This solution was homogenized ten times at 500 rpm using a tight fitting teflon homogenizer and centrifuged 5 min at 700 *g*. This pellet was resuspended in the same sucrose solution as above without Triton to obtain three times the original volume and centrifuged at 700 *g* for 5 min. This wash was repeated twice. The pellet was resuspended in 2 volumes of the same digestion buffer as used for chicken erythrocyte chromatin. Chromatin was extracted following the same procedure as for chicken erythrocyte nuclei. Similar procedures were followed for the preparation of chromatin fragments from Psammechinus miliaris obtained from the Biologische Anstalt Helgoland. In both cases, the chromatin fragments had on average 70–90 nucleosomes.

Results of histone analysis and linker length determination carried out as described earlier (Koch et al. 1987a) are illustrated in Fig. 1.

Solubility experiments

After extraction, chicken erythrocyte chromatin was first dialyzed overnight against TE buffer. This was followed by dialysis at twice the final chromatin concentration used in the experiments for at least 5 h against five changes of a buffer with 5 m*M* *Tris* · HCl, pH 7.5, with 0.1% NaN_3 or 0.5 m*M* PMSF (*Tris* buffer). The cation and chromatin stock solutions were all prepared immediately prior to use. After mixing, samples and reference solutions containing appropriate cation concentrations were left for at least 1 h at 4 °C followed by centrifugation of the samples for 10 min at 20,000 rpm (about 6,000 *g*) in a Beckmann Airfuge A100 rotor. Immediately after centrifugation, the supernatant and references were diluted in *Tris* buffer to give an absorption A_{260} in the range 0–1.0. The absorption of each sample was measured against its reference at 260 and 310 nm in a Zeiss DMR 10 spectrophotometer.

Effect of cations

For these experiments, chromatin in TE buffer was dialyzed against several changes of *Tris* buffer to eliminate EDTA from the solutions. Spermine · 4 HCl and Spermidine · 3 HCl (Serva) were added from 1–5 m*M* stock solutions in *Tris* buffer to final concentrations in the range 0–1.6 m*M* · $CrCl_3 \cdot 6\ H_2O$ (Merck) was added from a 2.5 m*M* stock solution in *Tris* buffer to chromatin solutions in the range 0–1 m*M*. $GdCl_3 \cdot 6\ H_2O$ (Aldrich Chemical Co) was dissolved at 2 m*M*

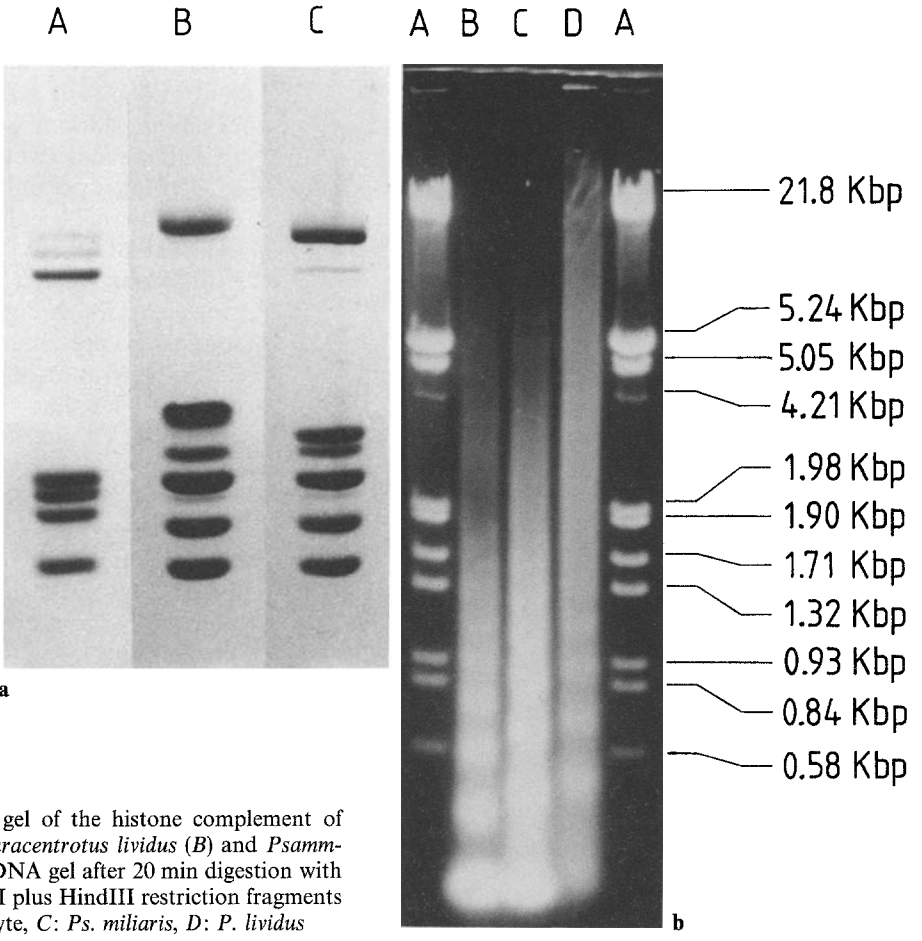

Fig. 1. a SDS polyacrylamide (15%) gel of the histone complement of chicken erythrocyte chromatin (*A*), *Paracentrotus lividus* (*B*) and *Psammechinus miliaris* (*C*). **b** Agarose (1.5%) DNA gel after 20 min digestion with Micrococcal nuclease. *Lane A*: ECO RI plus HindIII restriction fragments of phage λ DNA, *B*: chicken erythrocyte, *C*: *Ps. miliaris*, *D*: *P. lividus*

in *Tris* buffer and added to chromatin solutions to final concentrations in the range 0–1 m*M*. Similarly a 4 m*M* $TbCl_3$ stock solution was used to obtain final concentrations of 0–1.5 m*M*.

X-ray solution scattering

All experiments were performed on the double focusing monochromator mirror camera X33 (Koch and Bordas 1983) in HASYLAB on the storage ring DORIS of the Deutsches Elektronen Synchrotron (DESY) using a quadrant detector (Hendrix, Gabriel, Boulin unpublished) and data acquisition and evaluation systems described earlier (Boulin et al. 1986). The values of the radius of gyration of the cross-section (R_x) and of the extrapolated forward cross-section scattering ($I(0)_x$), which is proportional to the mass per unit length, were obtained from plots of $\log(sI(s))$ vs s^2, where $s = 2\sin\theta/\lambda$, 2θ is the scattering angle and λ the wavelength.

Electro-optical measurements

Chicken erythrocyte chromatin solutions prepared as described in TE buffer, were extensively dialyzed against dichroism buffer (0.3 m*M* NaCl, 0.2 m*M* *Tris* · HCl, pH 7.5, 3 μ*M* EDTA, 0.5 m*M* PMSF) which had been carefully degassed. The measurements were performed as described by Marquet et al. (1988) and references therein. Condensation of chicken erythrocyte chromatin with Spermine, $CrCl_3$ and $MgCl_2$ was followed at $A_{260} = 0.45$.

Results

X-ray scattering

Sea urchin chromatin. The repeat length determined from the DNA gel shown in Fig. 1 is 210 base pairs (bp) for chicken erythrocyte chromatin, 240 for *Psammechinus miliaris* and 250 for *Paracentrotus lividus*. The histone analysis of *Ps. miliaris* chromatin in Fig. 1 is in agreement with that of Widom et al. (1985).

Figure 2 illustrates the changes in the scattering pattern of *Ps. miliaris* upon increasing ionic strength. At low ionic strength the interference maximum is shifted to lower *s*-values than in chicken erythrocyte chromatin. The interference function illustrated in Fig. 3 was determined by dividing the scattered inten-

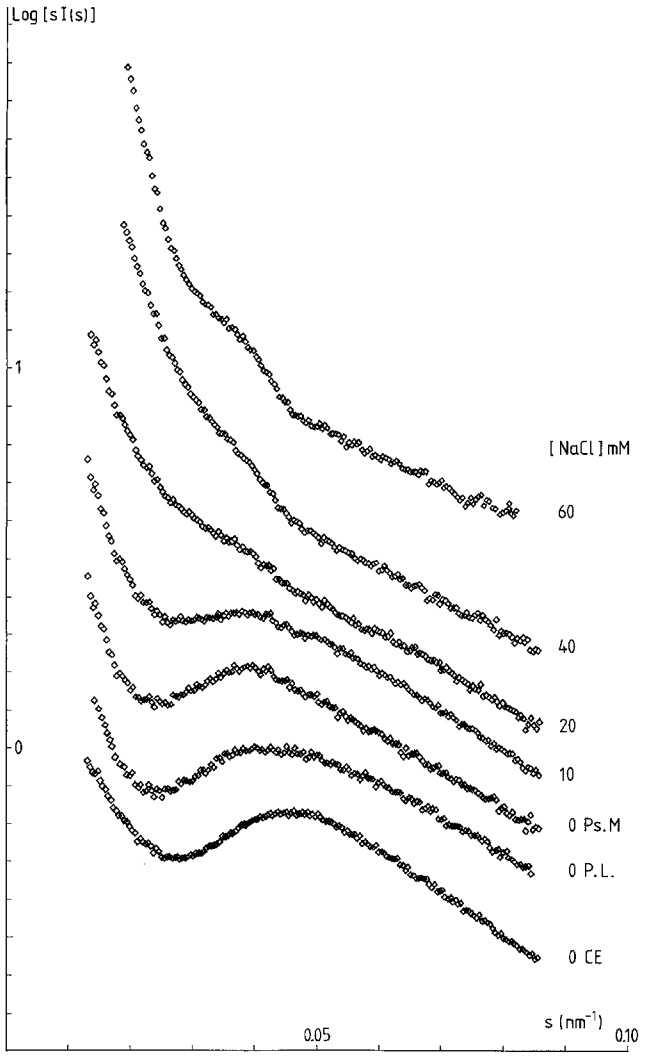

sity by the pattern obtained after prolonged digestion with micrococcal nuclease as described earlier (Koch et al. 1987 b). The average internucleosomal distance is 23 nm in chicken erythrocyte and about 30 nm in *Ps. miliaris* and *P. lividus* chromatin.

The mass per unit length of *Psammechinus miliaris* chromatin in TE buffer determined relative to *F*-actin (Koch et al. 1987 a; Greulich et al. 1987) is $28 \pm 2 \cdot 10^3$ daltons/nm. Taking an estimate of 310 kDa for the molecular weight of the repeating unit, this corresponds to approximately 1.0 nucleosome/11 nm. The radius of gyration of the cross-section is 14 nm, significantly higher than the value for chicken erythrocyte chromatin (10 nm) measured under identical conditions.

Above 20 m*M* NaCl a band develops in the scattering pattern at $s = 0.035\ \text{nm}^{-1}$. Precipitation occurs above 60 m*M* NaCl. The mass per unit length does not increase by more than a factor of 8 between 0 and 60 m*M* NaCl, when the first signs of precipitation occur.

Monovalent cations

The values of $\sqrt{I(0)_x}$ of chicken erythrocyte chromatin solutions as a function of the concentration of NaCl, NH_4Cl, $N(CH_3)_4Cl$ and $N(C_2H_5)_4Cl$ are

Fig. 2. Solution scattering pattern of chromatin fragments from *Psammechinus miliaris* (Ps. M) (2 mg DNA/ml) as a function of NaCl concentration. The *bottom curves* are the patterns of solutions of chicken erythrocyte (CE) and *Paracentrotus lividus* (P. L.) chromatin. The *curves* are displaced vertically for better visualization

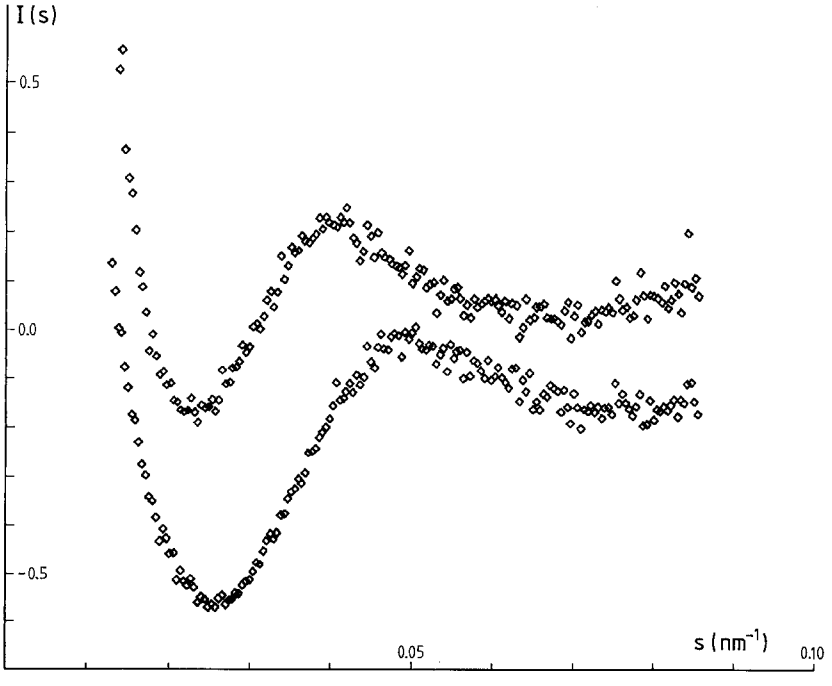

Fig. 3. Internucleosomal interference function for *Ps. miliaris* chromatin (*top*) and chicken erythrocyte chromatin (*bottom*) obtained by dividing the intensity of a solution of chromatin fragments (2 mg DNA/ml) by that of the same solution after prolonged digestion with micrococcal nuclease. The *lower curve* has been displaced vertically for better visualization

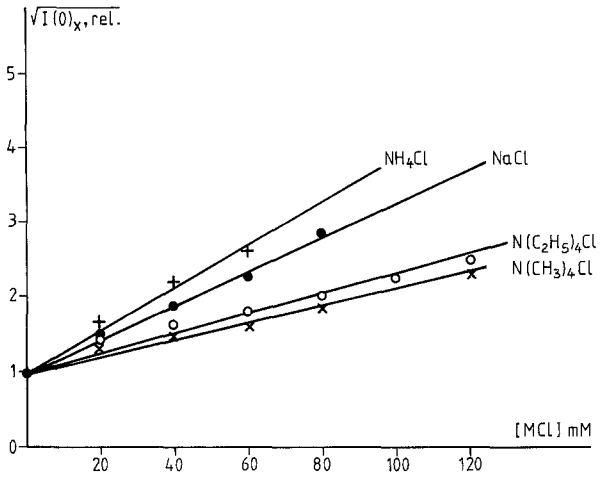

Fig. 4. Dependence of the $\sqrt{I(0)_x}$ for a solution of chicken erythrocyte chromatin fragments ($A_{260}=60$) on salt concentration for NaCl, NH_4Cl, $N(CH_3)_4Cl$ and $N(C_2H_5)_4Cl$

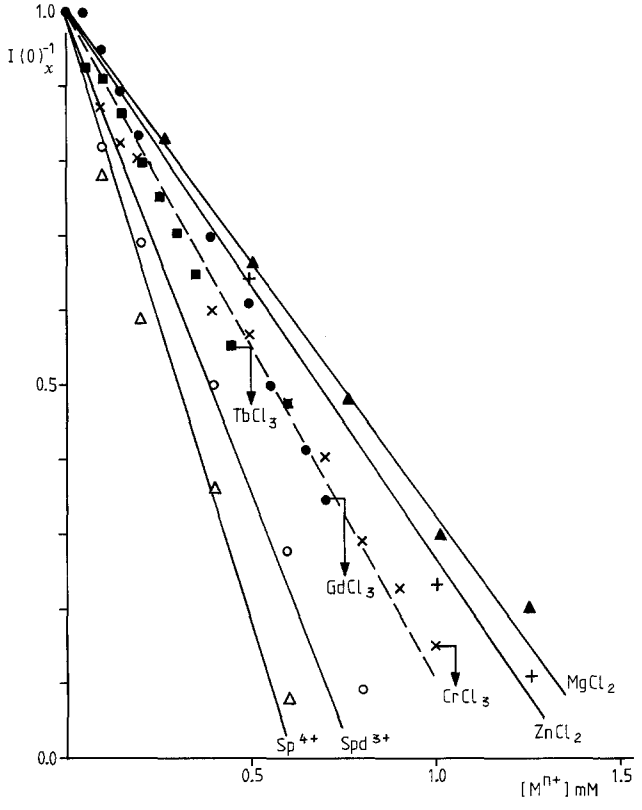

Fig. 5. Changes in the relative length of the chromatin fibers ($A_{260}=60$) as a function of cation concentration. The *arrows* indicate the concentrations beyond which precipitation occurs with trivalent cations

shown in Fig. 4. NH_4Cl is a more efficient condensation agent than NaCl which is in turn more efficient than the alkylammonium salts. There also appear to be small differences in the effect of salts with different anions (not shown), NaCl being more efficient than Na_2SO_4 and NaH_2PO_4. Ammonium sulphate is more efficient than sodium sulphate.

Divalent and multivalent cations

The decrease in relative length of the fibers, which is proportional to $I(0)_x^{-1}$, upon increasing cation concentration is illustrated in Fig. 5. The values for $MgCl_2$ at this chromatin concentration (2.5 mg DNA/ml) are given for comparison. $ZnCl_2$ is more efficient than $MgCl_2$ in condensing chromatin. The trivalent cations Tb^{3+}, Gd^{3+} and Cr^{3+} have similar effects on condensation. Compared to other cations, however, there is a very abrupt precipitation above a critical concentration. This critical concentration depends on the nature of the cation, as indicated by the arrows in Fig. 5. Reproducible results were obtained, especially with Gd^{3+}, only when using solutions from fresh reagents. The trivalent metal cations are less efficient condensation agents than spermidine (Spd^{3+}) and spermine (Sp^{4+}).

Solubility

The dependence of solubility on $MgCl_2$ concentration of solutions of chicken erythrocyte chromatin fragments in the concentration range $1 \leqslant A_{260} \leqslant 75$ is illustrated in Fig. 6. In all cases there is first a small increase in apparent absorbance followed by a rather sharp decrease in solubility. The concentration corresponding to the midpoint of the solubility curve increases approximately linearly in this range of chromatin concentration. Solubility curves in the presence of different cations at a fixed chromatin concentration ($A_{260}=20$) are shown in Fig. 7. Results (not shown) for other metal chlorides at a higher chromatin concentration ($A_{260}=40$) indicate that the efficiency of the cations as precipitating agents is Mn < Cd < Co < Ni < Zn and also confirm that for the earth alkali cations the order is Ba ≃ Sr ≃ Mg < Ca. Similar results (not shown) were also obtained by light scattering.

Electro-optical measurements

The dependence of the reduced dichroism of chicken erythrocyte chromatin on spermine concentration is illustrated in Fig. 8. In the absence of multivalent cations, the reduced dichroism is slightly negative. Extrapolation to infinite field yields a reduced dichroism of −0.135. The negative reduced dichroism decreases with spermine concentration and changes sign at a spermine/phosphate molar ratio of 0.12. The decrease in negative dichroism which accompanies condensation takes place before the onset of aggregation characterized by a rapid increase in turbidity. Similar effects were observed with $CrCl_3$ and $MgCl_2$ with a sign inversion at 0.09 m*M* Cr^{3+} and 0.45 m*M* Mg^{2+}

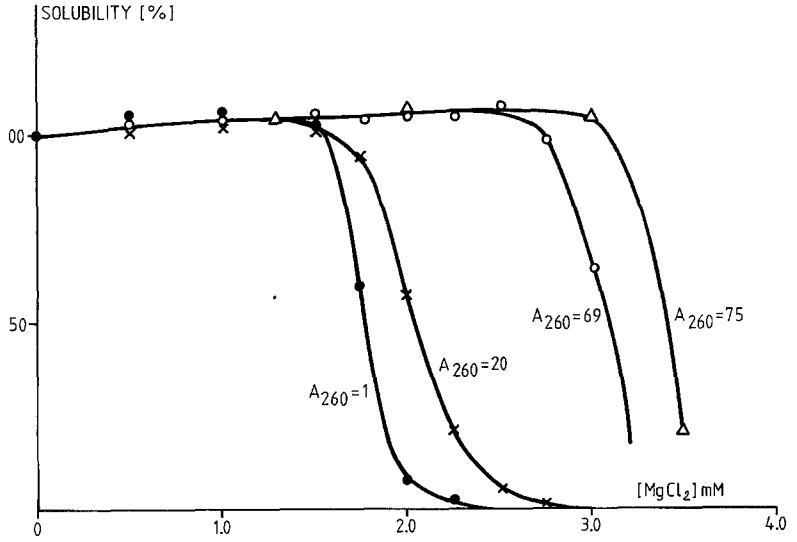

Fig. 6. Solubility of chicken erythrocyte chromatin as a function of $MgCl_2$ concentration at increasing chromatin concentrations

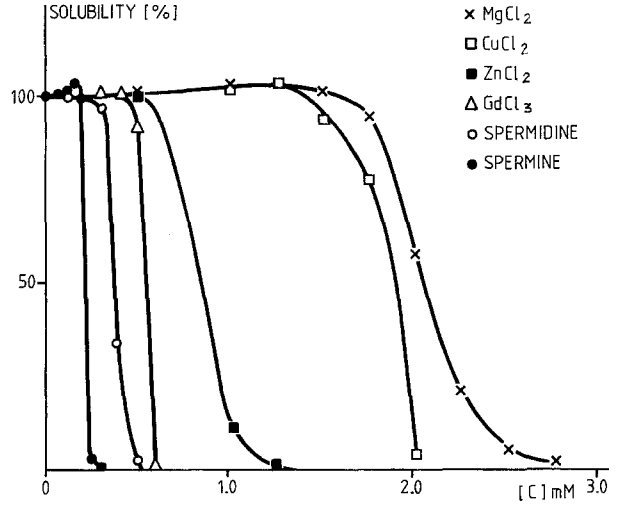

Fig. 7. Solubility of chicken erythrocyte chromatin ($A_{260}=20$) in the presence of various cations

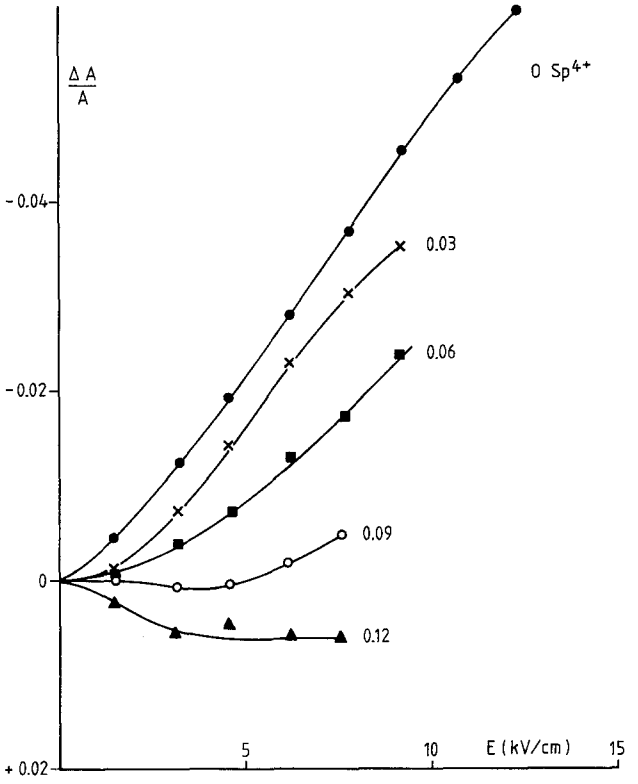

Fig. 8. Field strength dependence of the reduced dichroism of chicken erythrocyte chromatin at 260 nm for increasing spermine/phosphate concentration ratios in dichroism buffer

respectively. Fully condensed fibers displayed a positive dichroism in the range 0.01–0.04 with a saturation at fields above 6 kV/cm.

Discussion

The X-ray scattering results for sea urchin chromatin give further proof of the assignment of the band near 0.05 nm^{-1} in the scattering pattern at low ionic strength to the distance between successive nucleosomes (Koch et al. 1987b). The band which develops at 0.035 nm^{-1} in the log ($sI(s)$) vs s plots above 20 mM NaCl corresponds to the first side maximum of the fiber transform. A similar band has been observed at 0.045 nm^{-1} in the pattern of condensed chicken erythrocyte chromatin (Bordas et al. 1986a) and has been described in the pattern of nuclei in physiological salt conditions (Williams et al. 1986). Its origin is different from that of the band appearing in the range $s=0.025$ nm^{-1} in gels (Bordas et al. 1986a) and nuclei (Langmore and Paulson 1983; Bordas et al. 1986a; Notbohm 1986). The latter arises from the side by side packing of the condensed chromatin fibers.

Assuming a uniform cylinder, the fibers of sea urchin chromatin have an outer diameter of 40–45 nm.

This is in agreement with the value found by electron microscopy (45 nm) by Zentgraf and Franke (1984) and in contradiction with the electron microscopy results of Widom et al. (1985) who concluded that the diameter of the condensed fiber is independent of the linker length. A diameter around 45 nm is also consistent with the experimental value of the radius of gyration of the cross-section (16 nm). The interference band in nuclei and gels would then be expected to appear at *s*-values below 0.025 nm^{-1}. This is possibly why this band was not observed in sea urchin sperm nuclei (Langmore and Paulson 1983) or in oriented gels (Widom et al. 1985). Alternatively, as also suggested by the latter authors, the fibers are too closely packed to still give rise to this band. Precipitation of sea urchin chromatin at salt concentration around 70 m*M* was also observed by Widom et al. (1985).

The mass per unit length of the condensed fiber of chicken erythrocyte chromatin (Koch et al. 1987a; Greulich et al. 1987) and for sea urchin chromatin obtained by X-ray scattering before the onset of aggregation is between six and eight nucleosomes per 11 nm, in agreement with the electron microscopic determination of Thoma et al. (1979) on rat liver chromatin. Electron microscopic observations yield values up to 12 nucleosomes/11 nm for other echinoderm sperm chromatin (Williams et al. 1986). This suggests that full compaction in vitro is only achieved after the onset of precipitation. Extrapolation of the mass per unit length for sea urchin chromatin indicates that a value of 12 nucleosomes/11 nm would be obtained at 80 m*M* NaCl. Given the larger diameter of the fibers this would correspond to the same nucleosome packing density as in chicken erythrocyte fiber with 6–8 nucleosomes/11 nm. A value of 12 nucleosomes/11 nm was also recently obtained by sedimentation experiments on rat liver chromatin (Walker and Sikorska 1987). These authors also give an outer radius of 40 nm for the condensed fiber. It is however difficult to see how such a fiber could be formed with chromatin having only a linker of 34 bp crossing the central part of the fiber. The result contradicts the electron microscopic observations of Williams et al. (1986) and previous X-ray measurements (Koch et al. 1987a). The aggregation properties of rat liver chromatin above 80 m*M* NaCl suggest that the value may be on overestimate in this case.

The fact that there is a relationship between fiber diameter and linker length is an argument in favour of models in which the linker DNA runs across the central part of the fiber. The relationship between linker length and fiber diameter is not, however, an argument against solenoid or coil type models.

Although enzymatic digestion experiments (Staynov 1983; Drinkwater et al. 1987) have also been interpreted as resulting from the fact that successive nucleosomes in the chain are not adjacent in the 30 nm filament, the point cannot yet be considered to be entirely proven.

The effect of cations on the condensation confirm that at least in vitro, there are distinct processes of compaction and of aggregation as also suggested by Marquet et al. (1988). Some of the aspects of compaction of the fibers at low ionic strength and in particular the competitive effects of monovalent and divalent cations (Borochov et al. 1984; Widom 1986) can be explained in terms of the polyelectrolyte theory of Manning (1978). The empirical approach of Tam and Williams (1985) is, however, more useful in understanding how structural requirements introduce selectivity. In particular, the abrupt precipitation observed with Gd and Tb can be explained because the lanthanides have few requirements on coordination numbers, angles or bond lengths and thus easily cross-link the fibers. A similar explanation applies in the case of Cr and may also explain some of the differences between divalent cations. In general our results with monovalent cations (Koch et al. 1987a) do not confirm the observation of Tam and Williams (1985) that the larger cations would be more efficient in inducing compaction of the fibers.

The greater efficiency of ammonium chloride compared to NaCl and to the alkylammonium chlorides illustrates the importance of structural effects like hydrogen bonding, as opposed to charge, in determining the efficiency of condensing agents. This is further confirmed by the low levels at which the polyamines, spermine and spermidine, induce compaction. Although these studies have only a physicochemical relevance, they suggest that unless precautions are taken, negative staining in electron microscopy may easily result in cross-linking of the fibers. Furthermore they suggest a partial explanation for the very high toxicity of some heavy metals. Trivalent chromium, for instance, induces cross-links between nuclear proteins and DNA (Wedrychowski et al. 1985).

The results for Gd and the polyamines follow the same trends as those of Sen and Crothers (1986) obtained by electric dichroism, although the values of reduced dichroism obtained by this group for chicken erythrocyte chromatin are much more negative than ours (see below). Marquet et al. (1988) also found the same behaviour for the polyamines and Tb by electric dichroism but the values of the reduced dichroism for chicken erythrocyte chromatin were similar to ours.

The main purpose of the solubility experiments was to give a definite proof that the X-ray scattering measurements reflect compaction of the fibers and not aggregation. The experiments confirm the differences between cations observed by X-rays and are broadly in agreement with the results of Borochov et al. (1984). As already observed by Borochov et al. (1984) there is

an increase in turbidity corresponding to compaction of the fibers followed by the onset of aggregation. The results also show that contrary to a widespread belief (e.g., Widom 1986) at higher chromatin concentrations, there is an approximately linear dependence of the Mg^{2+} concentration at which precipitation sets in. This has a physiological relevance since chromatin concentrations in nuclei can be as high as 30 mg/ml (For a review, see Kellenberger 1987) or about five times higher than in most of our X-ray experiments or several hundred times higher than with optical techniques.

The values of the reduced dichroism in Fig. 8 further characterize our samples of chicken erythrocyte chromatin. They are in agreement with those found independently by Marquet et al. (1988) using slightly different preparative methods. For uncondensed chromatin the values (-0.02 at 6 kV/cm) are much less negative than those of McGhee et al. (1980) (-0.28) or of Sen and Crothers (1986) (-0.15) at the same field. Whereas our values for condensed chromatin are positive ($+0.04$) these authors still find negative values of -0.08 and -0.04 respectively. Previously, Lee et al. (1981) and Yabuki et al. (1982) had however reported positive values around $+0.05$ for condensed chromatin stabilized by cross-linking with dimethylsuberimidate. The experimental values of flow birefringence determined by Harrington (1985) for fractionated chicken erythrocyte chromatin are negative at low Na^+ or Mg^{2+} concentrations and positive for condensed chromatin. The intrinsic contribution obtained after correction for the form effects remains, however, negative throughout the range of condensation. In contrast with these results, Marion et al. (1985) found a positive birefrigence independently of the degree of condensation. Dimitrov et al. (1987) reported a reduced dichroism value of -0.10 at 5 kV/cm at very low ionic strength but a value of $+0.02$ value above 2 m*M* NaCl confirming the sign inversion previously detected by flow techniques (Makarov et al. 1985). For neuronal chromatin which has a short linker ($\leqslant 20$ base pairs), Allan et al. (1984) found a negative electric dichroism throughout the range of ionic strength whereas flow dichroism yields negative values at low ionic strength with a sign inversion around 10 m*M* NaCl in the case of Erlich ascite chromatin which also has a linker of about 20 base pairs (Kubista et al. 1985). The origin of these differences is still unknown.

The negative values for uncondensed chromatin in Fig. 8 are in agreement with our structural model (Bordas et al. 1986b; Koch et al. 1987a). The "beads on a string" model of McGhee et al. (1980), which corresponds to the more negative values observed by these authors gives values of the radius of gyration of the cross-section which are incompatible with the X-ray scattering results. For the condensed form the observed positive dichroism requires the linker to lie in the plane perpendicular to the fiber axis if one takes into account the preferential orientation of the nucleosomes determined from the scattering pattern of oriented gels (Widom and Klug 1985). A more detailed analysis of the consistency of the dichroism and X-ray scattering data will be presented elsewhere.

As shown earlier (Koch et al. 1987a), despite the fact that different conclusions may have been drawn, there is substantial agreement between the experimental X-ray data of several groups working on different types of chromatin. The solubility experiments prove that these results correspond to compaction of the fibers and not to aggregation. Our results also confirm other reports on the dependence of fiber diameter on linker length (Zentgraf and Franke 1984; Williams et al. 1986). The situation is different with electric and flow dichroism results where the contradictions could probably best be resolved by measurements using different techniques on the same samples. A stronger emphasis on consistency between the results of different methods would certainly help to narrow down the number of possible models for the structure(s?) of chromatin.

Acknowledgements. We thank Dr. H. Notbohm for the use of his light scattering equipment and Dr. J. F. Desreux for synthesising $TbCl_3$. R. M. was supported by a fellowship from the Federation of European Biochemical Societies (FEBS).

References

Allan J, Rau DC, Harborne N, Gould H (1984) Higher order structure in short repeat length chromatin. J Cell Biol 98:1320–1327

Ausio J, Borochov N, Seger D, Eisenberg H (1984) Interaction of chromatin with NaCl and $MgCl_2$: Solubility and binding studies, Transition to and characterization of the higher order structure. J Mol Biol 177:373–398

Bordas J, Perez-Grau L, Koch MHJ, Nave C, Vega MC (1986a) The superstructure of chromatin and its condensation mechanism. I: Synchrotron radiation X-ray scattering results. Eur Biophys J 13:157–174

Bordas J, Perez-Grau L, Koch MHJ, Nave C, Vega MC (1986b) The superstructure of chromatin and its condensation mechanism. II: Theoretical analysis of the X-ray scattering patterns and model calculations. Eur Biophys J 13:175–186

Borochov N, Ausio J, Eisenberg H (1984) Interaction and conformational changes of chromatin with divalent ions. Nucleic Acid Res 12:3089–3096

Boulin C, Kempf R, Koch MHJ, McLaughlin SM (1986) Data appraisal, evaluation and display for synchrotron radiation experiments: hardware and software. Nucl Instrum Methods A249:399–407

Dimitrov SI, Smirnov IV, Makarov VL (1988) Optical anisotropy of chromatin: Flow linear dichroism and electric dichroism studies. J Biomol Struct Dyn 5:1135–1148

Drinkwater RD, Wilson PR, Skinner JD, Burgoyne LA (1987) Chromatin structures: dissecting their patterns in nuclear digests. Nucl Acids Res 15:8087–8103

Finch JT, Klug A (1976) Solenoidal model for superstructure in chromatin. Proc Natl Acad Sci USA 73:1897–1901

Gerchman SE, Ramakrishnan V (1987) Chromatin higher order structure studied by neutron scattering and scanning transmission electron microscopy. Proc Natl Acad Sci USA 84: 7802–7806

Greulich KO, Wachtel E, Ausio J, Seger D, Eisenberg H (1987) Transition of chromatin from the "10 nm" lower order structure, to the "30 nm" higher order structure, as followed by small angle X-ray scattering. J Mol Biol 193:709–721

Harrington RE (1985) Optical model studies of the salt induced 10–30 nm fiber transition in chromatin. Biochemistry 24: 2011–2021

Kellenberger E (1987) The compactness of cellular plasmas; in particular chromatin compactness in relation to function. TIBS 12:105–107

Koch MHJ, Bordas J (1983) X-ray diffraction and scattering on disordered systems using synchrotron radiation. Nucl Instrum Methods 208:461–469

Koch MHJ, Vega MC, Sayers Z, Michon AM (1987a) The superstructure of chromatin and its condensation mechanism. III: Effect of monovalent and divalent cations X-ray solution scattering and hydrodynamic studies. Eur Biophys J 14: 307–319

Koch MHJ, Sayers Z, Vega MC, Michon AM (1987b) The superstructure of chromatin and its condensation mechanism. IV: Enzymatic digestion, thermal denaturation, effect of netropsin and distamycin. Eur Biophys J 15:133–140

Kubista M, Hard T, Nielsen PE, Norden B (1985) Structural transitions of chromatin at low salt concentrations: A flow linear dichroism study. Biochemistry 24:6336–6342

Langmore JP, Paulson JR (1983) Low angle X-ray diffraction studies of chromatin structure in vivo and in isolated cell nuclei and metaphase chromosomes. J Cell Biol 96:1120–1131

Makarov V, Dimitrov S, Smirnov V, Pashev I (1985) A triple helix for the structure of chromatin fiber. FEBS Lett 181: 357–361

Manning GS (1978) The molecular theory of polyelectrolyte solutions with applications to the electrostatic properties of polynucleotides. Qu Rev Biophys 11:179–246

Marion C, Martinage A, Tirard A, Roux B, Daune M, Mazen A (1985) Histone phosphorylation in native chromatin induces local structural changes as probed by electric birefringence. J Mol Biol 186:367–379

Marquet R, Colson P, Matton AM, Houssier C, Thiry M, Goessens G (1988) Comparative study of the condensation of chicken erythrocyte and calf thymus chromatins by di- and multivalent cations. J Biol Struct Dyn 5:839–857

McGhee JD, Rau DC, Charney E, Felsenfeld G (1980) Orientation of the nucleosome within the higher order structure of chromatin. Cell 22:87–96

Lee KS, Mandelkern M, Crothers DM (1981) Solution structural studies of chromatin fibers. Biochemistry 20:1438–1445

Notbohm H (1986) Small angle scattering of cell nuclei. Eur Biophys J 13:367–372

Perez-Grau L, Bordas J, Koch MHJ (1984) Synchrotron radiation X-ray scattering study on solutions and gels. Nucleic Acids Res 12:2987–2995

Ramsay-Shaw B, Schmitz KS (1976) Quasielastic light scattering by biopolymers. Conformation of chromatin multimers. Biochem Biophys Res Commun 73:224–232

Sayers Z (1988) Synchrotron X-ray scattering studies of the chromatin fiber structure. In: Mandelkow E (ed) Synchrotron radiation in chemistry and biology, I. Springer, Berlin Heidelberg New York (Topics in current chemistry, vol 145, pp 203–232)

Sen D, Crothers DM (1986) Condensation of Chromatin: Role of Multivalent Cations. Biochemistry 25: 1495–1503

Staynov DZ (1983) Possible nucleosome arrangements in the higher order structure of chromatin. Int J Biol Macromol 5:3–9

Subirana JA, Munoz-Guerra S, Aymami J, Radermacher M, Frank J (1985) The layered organization of nucleosomes in 30 nm fibers. Chromosoma 91:377–390

Tam SC, Williams RJP (1985) Electrostatics and biological systems. Struct Bonding 63:103–151

Thoma F, Koller T, Klug A (1979) Involvement of histone H1 in the organization of the nucleosome and of the salt dependent superstructures of chromatin. J Cell Biol 83:403–407

Walker PR, Sikorska M (1987) Chromatin structure: Evidence that the 30 nm fiber is a helical coil with 12 nucleosomes/turn. J Biol Chem 262:12223–12227

Wedrychowski A, Ward WS, Schmidt WN, Hnilica LS (1985) Chromium-induced cross-linking of nuclear proteins and DNA. J Biol Chem 260:7150–7155

Widom J (1986) Physicochemical studies of the folding of the 100 Å nucleosome filament into the 300 Å filament. J Mol Biol 190:411–424

Widom J, Klug A (1985) Structure of the 300 A filament: X-ray diffraction from oriented samples. Cell 43:207–213

Widom J, Finch JT, Thomas JO (1985) Higher order structure of long repeat chromatin. EMBO J 4:3189–3194

Williams SP, Athey BD, Muglia LJ, Schappe R, Gough AJ, Langmore JP (1986) Chromatin fibers are left-handed double helices with diameter and mass per unit length that depend on linker length. Biophys J 49:233–250

Yabuki H, Dattagupta N, Crothers DM (1982) Orientation of nucleosomes in the thirty-nanometer chromatin fiber. Biochemistry 21:5015–5020

Zentgraf H, Franke WW (1984) Differences of supranucleosomal organization in different kinds of chromatin: Cell type-specific globular subunits containing different numbers of nucleosomes. J Cell Biol 99:272–286